ON THE CORONAL LINES λ5303 Å AND λ6374 Å

A. PERAIAH and B. A. VARGHESE

Indian Institute of Astrophysics, Bangalore 560034, India

(Received 30 July, 1986; in revised form 20 June, 1989)

Abstract. We present theoretical calculations of the observed coronal emission line profiles of Fe XIV (5303 Å) and Fe X (6374 Å) ions, which are observed at the time of total solar eclipse. Baumbach's relation (Allen, 1973) of electron density has been employed to compute the full width at half maximum FWHM. We have employed several other electron density distributions and found that the calculated differences in the FWHM are within 0.5% of one another. We have used the ion densities N_i/N_E given by Jordan (1969). To explain the observed FWHM, we have assumed that the corona is expanding spherically symmetrically with a velocity of one or two mean thermal units and no turbulence is included. With these highly simplified assumptions, we have reproduced qualitatively the profiles and FWHM's of the above lines. However, to explain quantities of FWHM's, we should take into account the inhomogeneities in the structure of the corona. It is thus shown, that turbulence is not necessary to explain the observed FWHM.

1. Introduction

It is customary to estimate the coronal temperature by using the full width at half maximum (FWHM) of the iron lines λ5303 Å (Fe XIV) and λ6374 Å (Fe X) (see Figures 1 and 2) that are observed at total solar eclipses (see Singh, Bappu, and Saxena, 1982; Desai and Chandrasekhar, 1983) by employing the formula (Aller, 1963)

$$\delta\lambda_a = 2\sqrt{\ln 2}\,\frac{\lambda}{C}\,\alpha = 7.16 \times 10^{-7}\,\lambda\sqrt{T/M}\,,$$

where $\delta\lambda_a$ is the FWHM, C is the velocity of light, λ is the wavelength, T is the kinetic temperature in absolute units, and M is the atomic weight. However, the temperatures that are derived by substituting the observed widths in the above equation are usually very large. These high temperatures are not in agreement with those found by other methods. Therefore, an *ad hoc* assumption of turbulence is introduced to explain the large widths of these lines. What one normally does, is to write that

$$\alpha^2 = \left(\frac{2kT}{M}\right) + \xi^2\,,$$

where ξ is the turbulent velocity and k is the Boltzmann constant, instead of

$$\alpha = \left(\frac{2kT}{M}\right)^{1/2}\,.$$

One adjusts by trial and error, the values of T and ξ in such a way that the observed value of $\delta\lambda_a$ is satisfied by using the above relation. Although, because of high Reynolds numbers, one can expect turbulence in the corona, it is difficult to see how it affects the

Solar Physics **124:** 53–72, 1989.

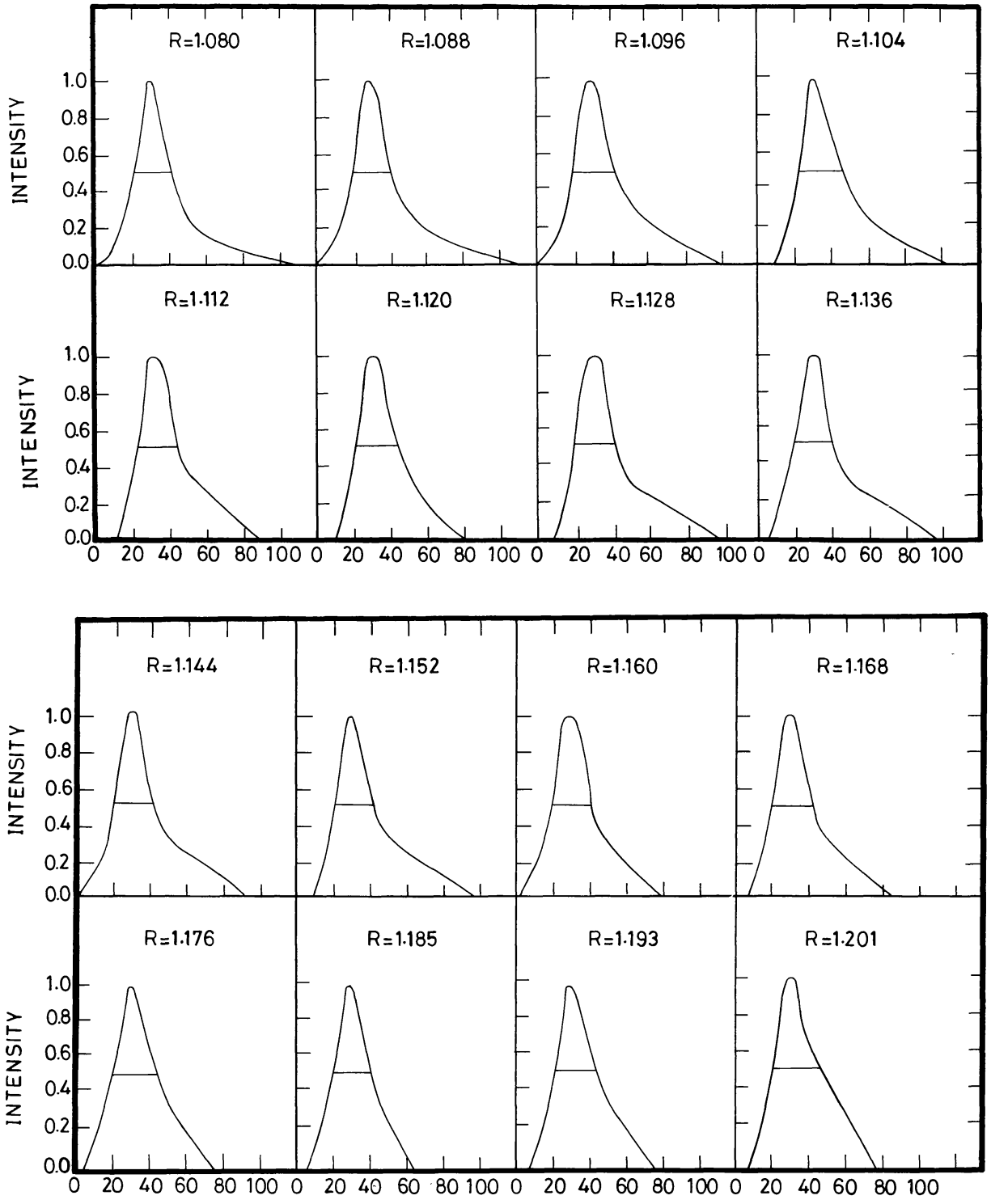

Fig. 1. Profiles of the λ5303 Å line, observed at the eclipse in Indonesia. Intensity measurements are accurate to within 2%. These are free-hand drawn curves fitted with a Gaussian. FWHM is marked at the middle of the profile. Intensities are normalized to the peak intensity.

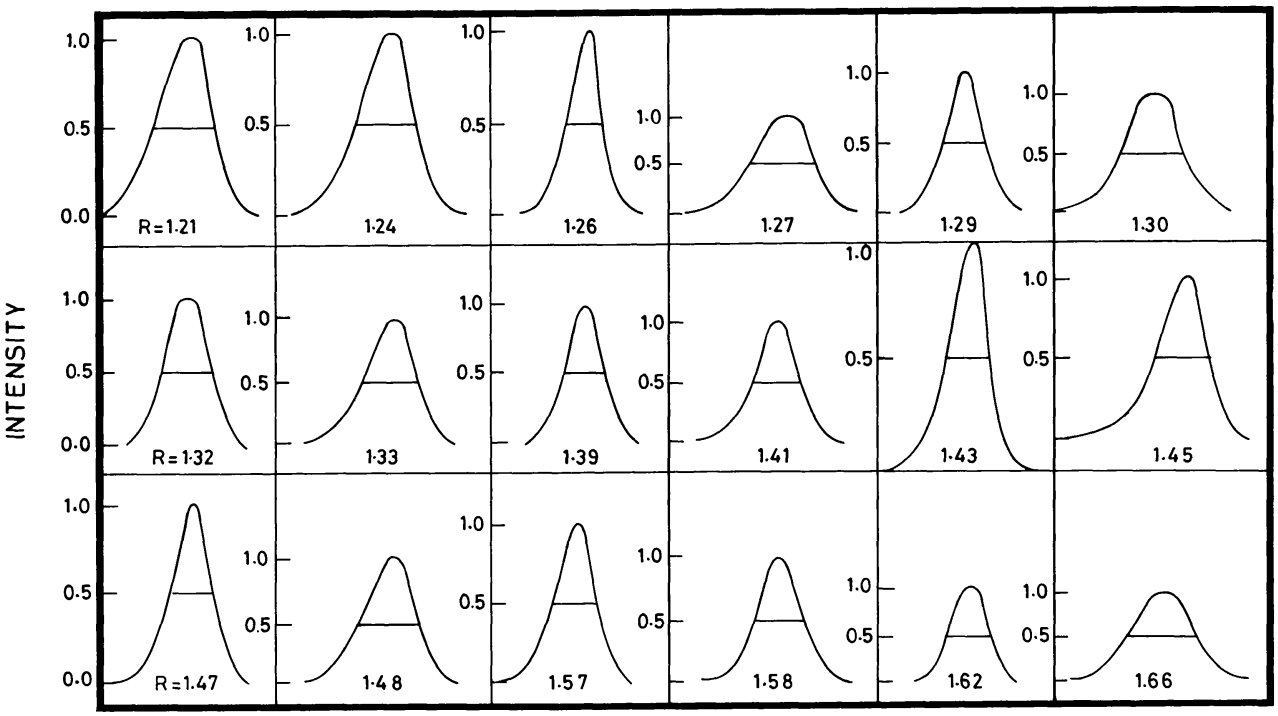

Fig. 2. Profiles of the λ6374 Å line, observed at the 1980 eclipse at Jwalagiri, India. Measurements are accurate to within 2%. Free-hand drawn curves fitted with Gaussian. FWHM is marked at the middle of the profile. Intensities are normalized to the peak intensity.

line-forming process (see, for example, Traving, 1975). The way turbulent velocities are introduced in calculating the widths of these lines is quite arbitrary. We feel, therefore, that there is enough reason for making an attempt to calculate the widths of the coronal lines λ5303 Å and λ6374 Å by taking account of the geometry, variation of the electron density, temperature gradients, and an expanding spherically symmetric corona. We would like to see whether or not a radial expansion of corona (Mihalas, 1978) can produce the observed profiles and FWHM. This is only a preliminary study and some of the physical assumptions need not be accurate in this context. A detailed study is under investigation.

In Figures 1 and 2, we present the observed profiles for λ5303 Å and λ6374 Å, respectively. The FWHM values are given in Table I. The intensities are normalized to the maximum in both cases. A glance at the FWHM values in Table I will show us that there is no correlation with the radius. This behaviour is perhaps due to the inhomogeneous distribution of matter.

2. Calculations

The calculations of the lines require the knowledge of the f-values, ion density, electron density, emission and absorption coefficients, and temperature variation in the corona. The electron density $N_e(r)$ is taken following the formula of Baumbach (Allen, 1973).

TABLE I

Observed values of FWHM for the λ5303 Å and λ6374 Å lines

λ5303 Å		λ6374 Å	
$R/R_\odot$	FWHM (Å)	$R/R_\odot$	FWHM (Å)
1.08	0.737	1.21	2.08
1.088	0.763	1.24	2.12
1.096	0.936	1.26	1.38
1.104	0.876	1.27	2.38
1.112	0.854	1.29	1.57
1.120	0.884	1.30	2.15
1.120	0.884	1.32	1.72
1.128	0.858	1.33	1.92
1.136	0.854	1.39	1.59
1.144	0.798	1.41	1.72
1.152	0.823	1.42	1.54
1.160	0.810	1.43	1.65
1.168	0.841	1.45	1.75
1.176	0.923	1.47	1.66
1.185	0.815	1.48	1.80
1.193	0.876	1.57	1.65
1.201	0.962	1.58	1.49
		1.62	1.43
		1.66	2.32

This is given by

$$N_e(r) = 10^8(0.036r^{-1.5} + 1.55r^{-6} + 2.99r^{-16})\ \mathrm{cm}^{-3}\,. \tag{1}$$

We have also considered the models due to Newkirk (1967). The values of FWHM obtained by different electron density distributions do not differ from those obtained by using the relation (1) by more than 0.5%. The temperature of quiet corona is considered and is taken from Allen (1973). The electron density and the temperature variations are plotted in Figure 3.

The wavelengths of the lines are λ5303 Å (Fe XIV) and λ6374 Å (Fe X). The f-values are calculated from the relation (see Aller, 1963)

$$f_{12} = 1.5 \times 10^8 \lambda_\mu^2 \frac{g_1}{g_2} A_{21}\,, \tag{2}$$

where the subscripts 1, 2 represent the lower and upper levels, respectively. λ_μ is the wavelength measured in microns. For λ = 6374 Å (Fe XIV) the values of g_1, g_2, and A_{21} are 4, 3, and 69 s^{-1}, respectively, and for λ = 5303 Å (Fe X), the values of g_1, g_2, and A_{21} are 2, 4, and 60 s^{-1}, respectively. The values of A's are taken from Allen (1973).

We assume a steady-state corona. For the sake of simplicity we shall also assume a two-level atom approximation although it may not be accurate in the present case. We

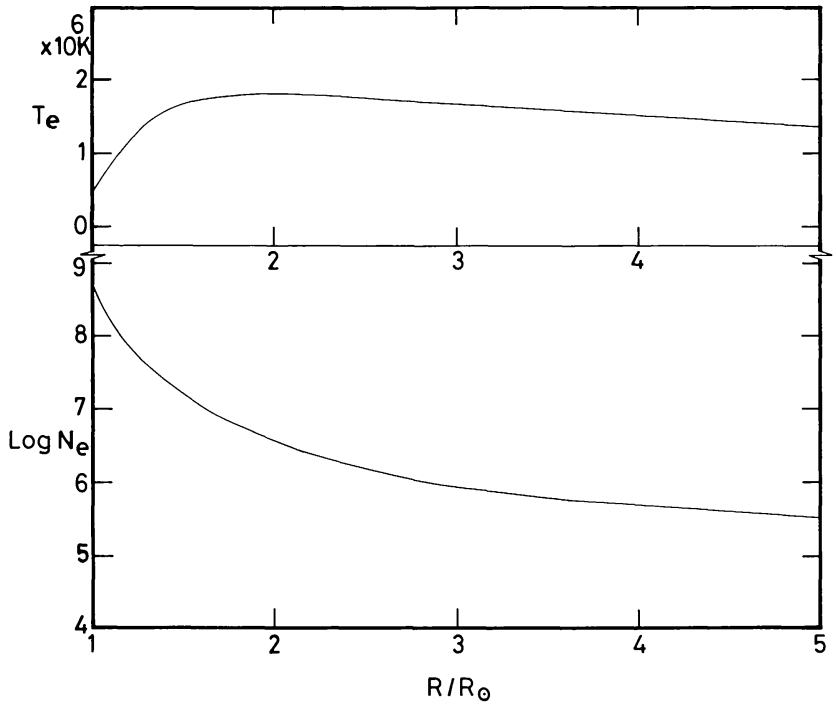

Fig. 3. Lower part of the figure is the run of electron density N_e according to Baumbach's relation. The upper part of the figure gives the run of temperature in the quiet corona. The data are taken from Allen (1973).

expect that the results obtained by this approximation may not differ much from the accurate results. From this point of view we shall write the statistical equilibrium equation as

$$n_1(R_{12} + C_{12}N_e) = n_2(A_{21} + R_{21} + C_{21}N_e)\,, \tag{3}$$

where R_{12} and C_{12} are, respectively, the radiative and collisional excitation rates and R_{21} and C_{21} corresponding de-excitation rates. n_1 and n_2 are the number densities of the levels 1 and 2, respectively. Since we do not consider other levels, n_1 and n_2 must satisfy the relation

$$n_1 + n_2 = n_{\text{ion}}\,. \tag{4}$$

This equation is very sensitive to the hypothesis that other level populations are negligible. Although this hypothesis is not exact we may get an order of magnitude estimate and this can be used until more accurate results are available. The quantities R_{12} and C_{12} are given by

$$R_{12} = \frac{g_2}{g_1} A_{21} \frac{1}{\exp\left\{\dfrac{1.44 \times 10^8}{\lambda(A) T_R(r)}\right\} - 1}\,, \tag{5}$$

where

$$T_R(r_0) = 5973 \text{ K} \quad \text{for Fe XIV},$$

$$T_R(r_0) = 5863 \text{ K} \quad \text{for Fe X},$$

and r_0 is the solar radius.

These temperatures are calculated by Raju (1985) from the solar fluxes given in Allen (1973).

Further, $T_R(r)$ is determined by assuming that

$$B_\nu(T_R(r)) = \left(\frac{r_0}{r}\right)^2 B_\nu(T_R(r_0)), \tag{6}$$

where B_ν is the Planck function. This gives us

$$T_R(r) = \frac{h\nu}{k} \frac{1}{\ln\left[1 + \left(\frac{r}{r_0}\right)^2 (e^{h\nu/kT(r_0)} - 1)\right]}, \tag{7}$$

where r is the radius of a shell in the corona. The quantity C_{12} is given by (Mason, 1975)

$$C_{12} = 8.63 \times 10^{-6} \Omega_{12} \exp\left\{\frac{-1.44 \times 10^8}{\lambda(A) T_R(r)}\right\} + 0.8 \times 1.39 \times 10^{-9}, \tag{8}$$

where

$$\Omega_{12} = 2.84 \quad \text{for Fe XIV},$$

$$\Omega_{12} = 1.62 \quad \text{for Fe X}.$$

Furthermore (Mihalas, 1978)

$$C_{21} = \frac{g_1}{g_2} C_{12} \exp\left[\frac{1.44 \times 10^8}{\lambda(A) T_R(r)}\right], \tag{9}$$

$$R_{21} = \frac{g_1}{g_2} R_{12}. \tag{10}$$

The emission coefficient is given by

$$\varepsilon = \frac{n_2 A_{21} h\nu}{4\pi}, \tag{11}$$

where n_2 is given by

$$n_2 = \frac{n_2}{n_{\text{ion}}} \frac{n_{\text{ion}}}{n_E} \frac{n_E}{n_{\text{H}}} n_{\text{H}}, \tag{12}$$

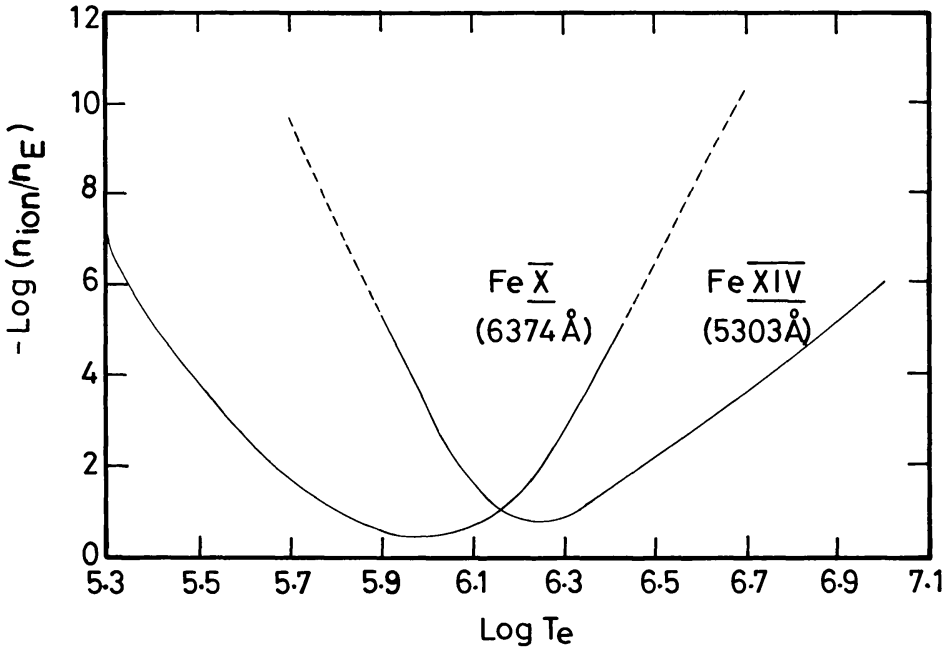

Fig. 4. The variation of $\log T_e$ with $-\log n_{\text{ion}}/n_E$ for the Fe XIV and Fe X ions. The data are taken from Table X of Jordan (1969).

where n_{ion}/n_E is the fractional ion abundance, n_E/n_{H} is the elemental abundance equal to 7×10^{-5}, and n = hydrogen density = $0.8N_e$. The quantity n_{ion}/n_E is taken from Table X of Jordan (1969) and is shown for both ions in Figure 4. Following Equations (3), (4), and (12) we can write Equation (11) as

$$\varepsilon_\nu = \frac{h\nu}{4\pi} A_{21} \frac{n_2}{n_{\text{ion}}} \frac{n_{\text{ion}}}{n_{\text{H}}} (0.8N_e), \tag{13}$$

where

$$n_2 = n_1 \left[\frac{R_{12} + N_e C_{12}}{R_{21} + A_{21} + N_e C_{21}} \right]. \tag{14}$$

The absorption coefficient in the line is given by

$$K_\nu = \frac{\pi e^2}{mC} \frac{f}{\sqrt{\pi}} \frac{n_1}{\Delta_{\text{D}}} F(x, r) \left(1 - \frac{n_2 g_1}{n_1 g_2} \right), \tag{15}$$

where e and m are the electronic charge and mass, respectively, and

$$F(x, r) = \frac{1}{\delta(r)} e^{-x^2/\delta^2(r)}, \qquad x = \frac{\nu - \nu_0}{\Delta_{\text{D}}}, \qquad \delta(r) = \Delta_{\text{D}}(r)/\Delta_{\text{D}} \tag{16}$$

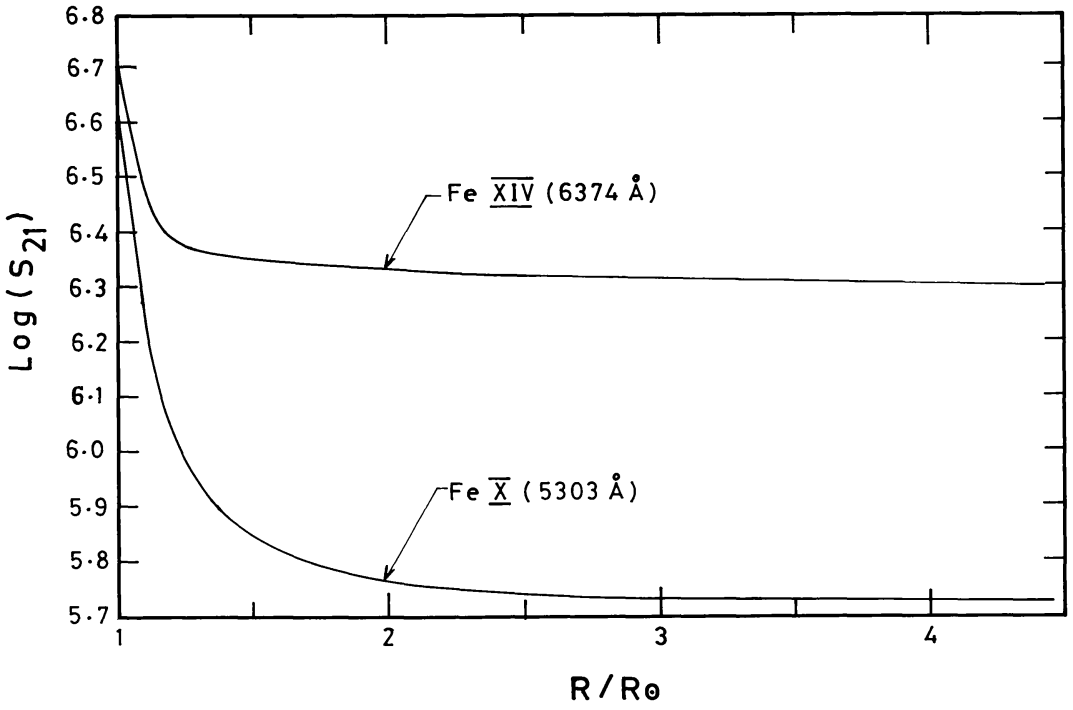

Fig. 5. Variation of the source functions with radius calculated according to Equation (18) in the text.

(see Rybicki, 1970); Δ_D is the Doppler width given by

$$\Delta_D = \frac{v_0}{c}\left(\frac{2k\overline{T}}{m_i}\right)^{1/2},$$

where $\overline{T}$ is the weighted average temperature defined as

$$\overline{T} = \sum_i r_i T(r_i) \Big/ \sum_i r_i ; \tag{17}$$

here $T(r_i)$ is the temperature at r_i (see Figure 3) and m_i is the mass of the iron ion. The line source function is given by

$$S_{21} = \frac{2hv^3}{c^2}\left[\frac{n_1 g_2}{n_2 g_1} - 1\right]^{-1}. \tag{18}$$

We have considered the contribution of the continuum radiation to the emission by electron scattering. It is found that the coronal continuum contribution to the emission is negligible within the range of 3 to 4 Doppler widths from the centre of the line. The specific intensities of the line at different widths (x) are calculated along the path of the rays as shown in Figure 6. No incident radiation is given at F and the intensity is calculated by using the formula (see Peraiah, 1980)

$$I_Q = I_P \exp\left[-\tau(PQ) + \int_P^Q S_{21}(t) \exp\left[-\{\tau(PQ) - t\}\right]\right] dt, \tag{19}$$

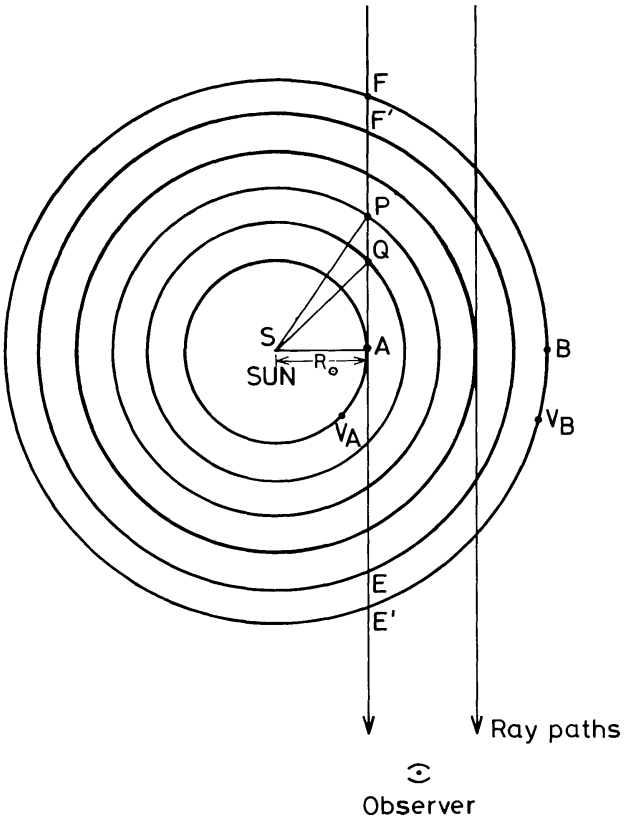

Fig. 6. Schematic diagram of the geometry of the corona showing how the lines are calculated.

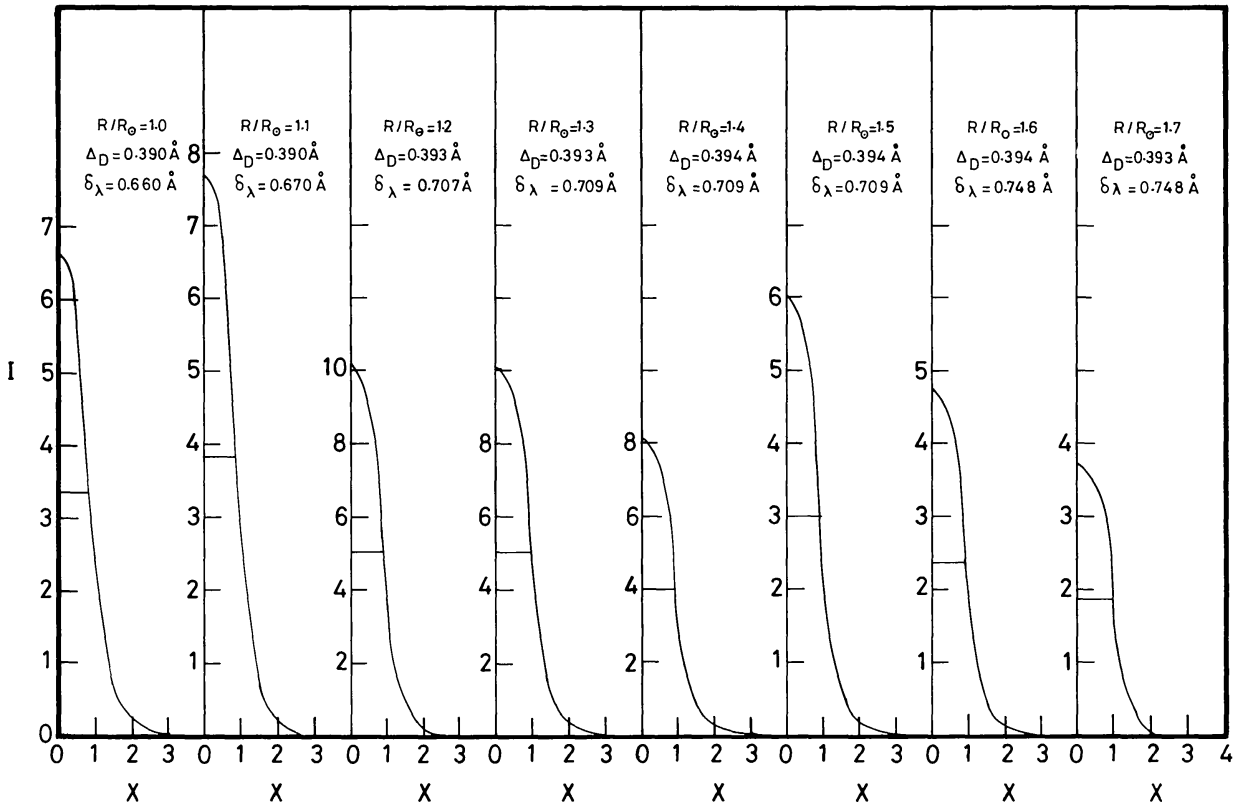

Fig. 7. Profiles of the λ5303 Å line with $V_E = 0$. We plotted half of the line because the profiles are symmetric.

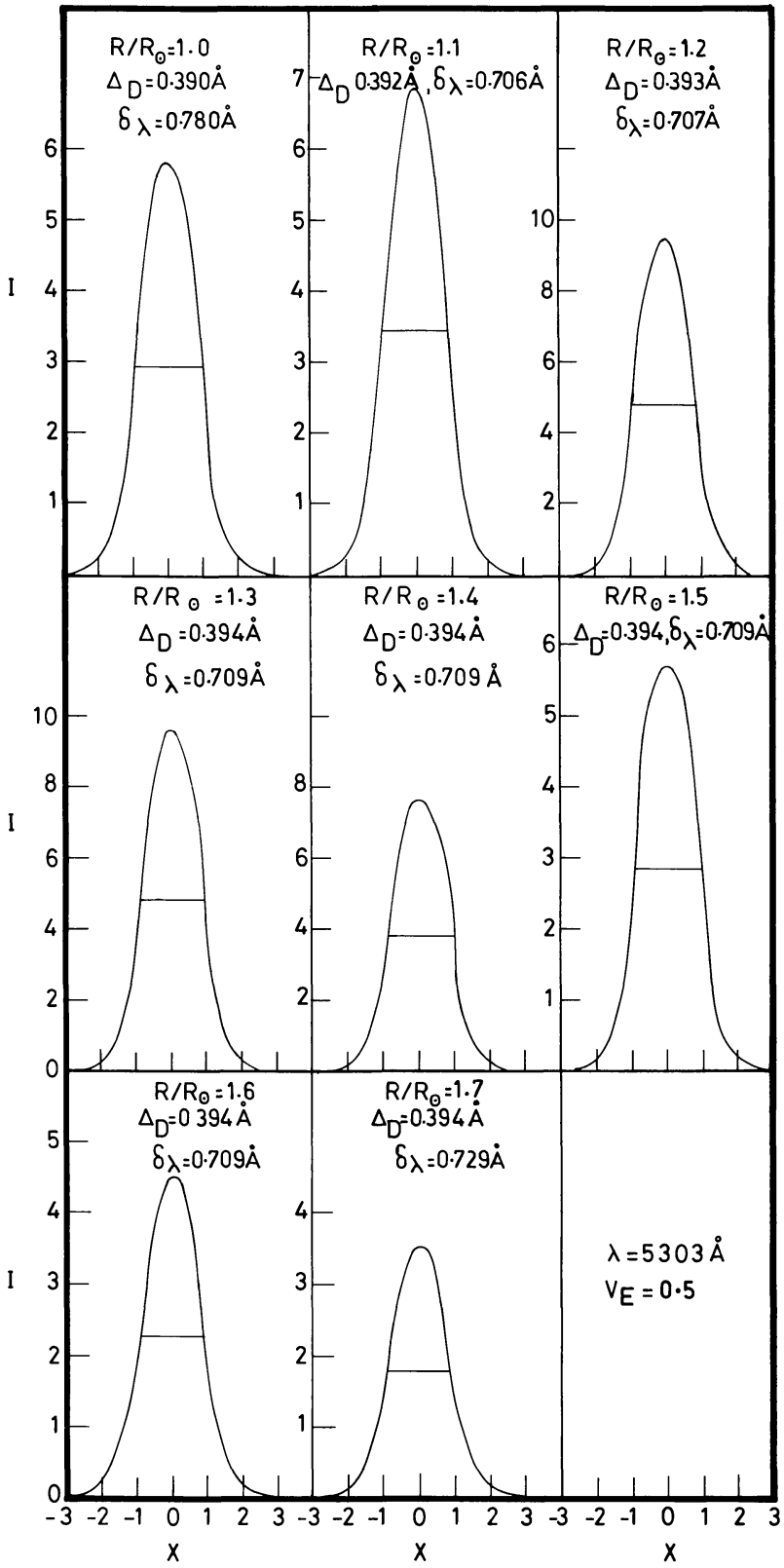

Fig. 8. Same as Figure 7, but with V_E = 0.5 Doppler units.

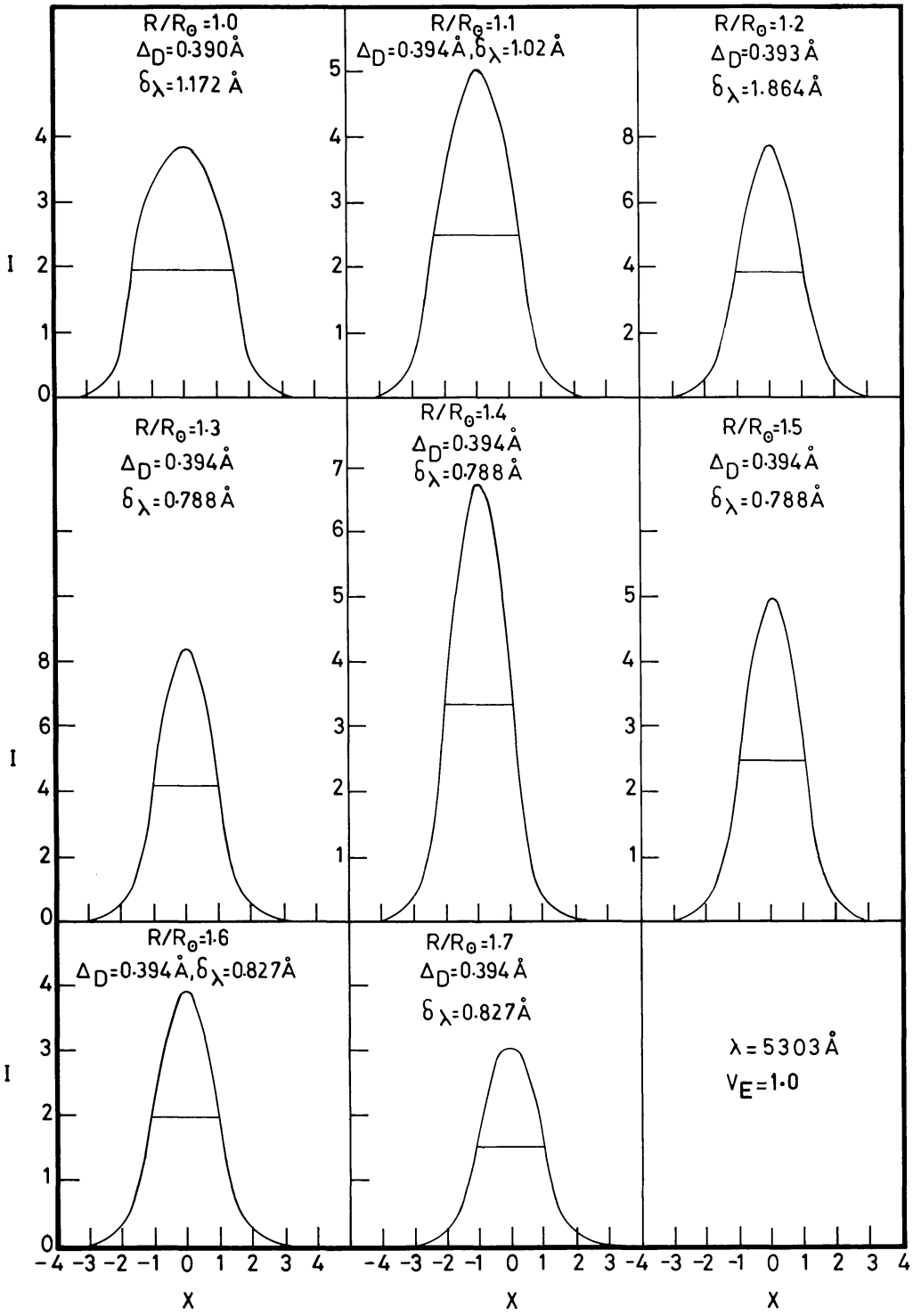

Fig. 9. Same as Figure 7, but with V_E = 1.0 Doppler units.

where I_P is the incident intensity, S_{21} is the source function, and $\tau(PQ)$ is the total optical depth in PQ. Equation (19) is repeatedly used in all the shells along the path of the ray from FF' until the last shell distance EE'. We calculated the intensities at each $\lambda_0 \pm \Delta\lambda$ in the line. The bandwidth is taken to be $\pm\beta$ where $\beta = 4$ or 5 times the standard Doppler width Δ_D.

If the corona is expanding (see Mihalas, 1978; Chandrasekhar, Desai, and Angreji, 1981), we should take into account the effects of expansion. In this case the bandwidth becomes $\pm(\beta + V)$, where V is the velocity of expansion in standard Doppler widths. The integral in Equation (19) is evaluated over each shell such as PQ. The velocities are introduced into the optical depth through the Doppler profile function $F(x, r)$ in Equation (16). Since we are dealing with corona in which temperature gradients exist, the Doppler width is not constant. Equation (16) takes care of the temperature gradients as the line forms at each radial point. We divided the corona into 70 spherical shells and each with equal radial thickness and the total geometrical thickness of corona is 5 $R_\odot$. It is assumed that matter beyond the radial thickness of 5 $R_\odot$ contributes little to the intensity of the rays along the line of sight. The radial distribution of electron density, the ion density and temperature are taken from the data given in Figures 3 and 4. The obtained lines for different cases and ray paths (given by $R_\odot$ in Figure 6) are plotted in Figures 7, 8, and 9 for λ5303 Å. In these figures we presented the lines for $R/R_\odot$ = 1 to 1.7. Here Δ_D is the standard Doppler width in ångstrom units and δ_λ is the full width at half maximum shown as a horizontal line at half maximum.

In Figure 7, we plotted the half profile of the line formed in a static corona. The FWHM are of the order of 0.7 Å where, as in Figure 1, we notice that the FWHM's vary around 0.8 or 0.9. Therefore, we introduced expansion velocities V_E of the order of 0.5 and 1.0 standard Doppler unit. The corresponding profiles are described in

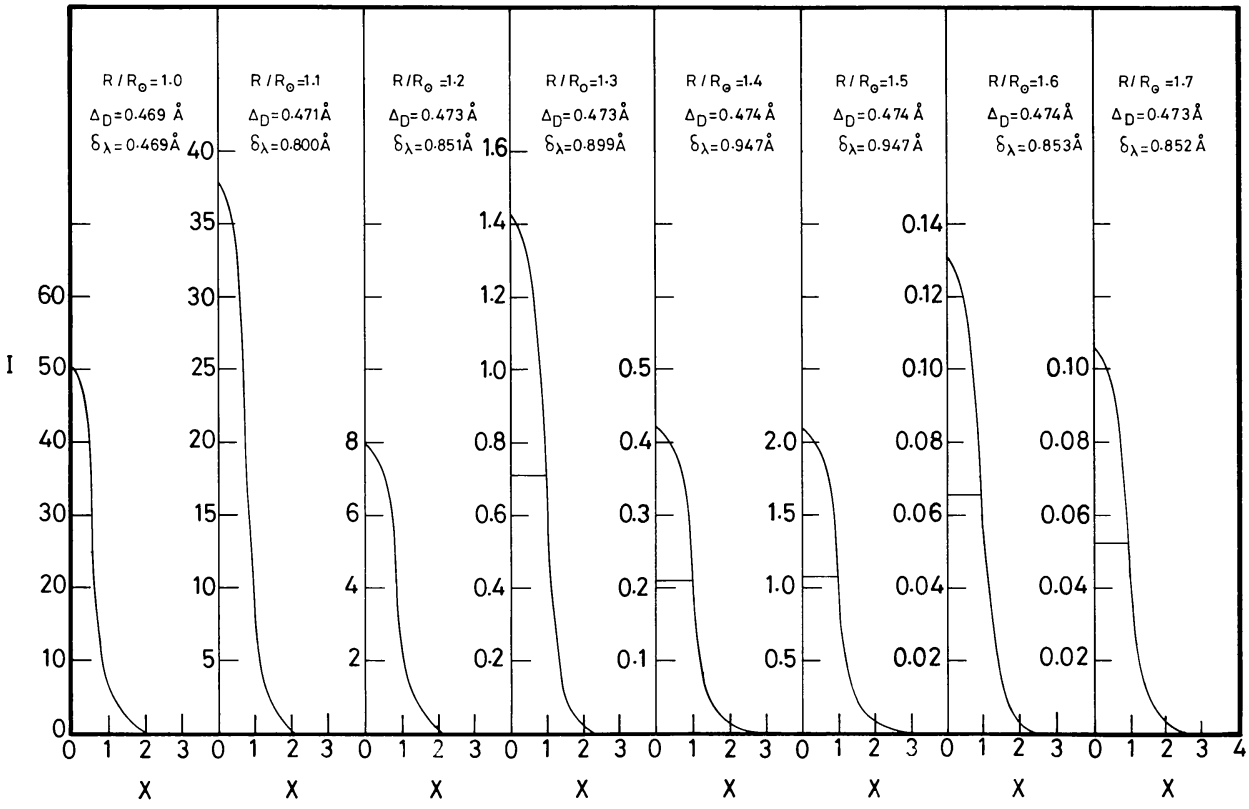

Fig. 10. Profiles of the λ6374 Å line with V_E = 0.

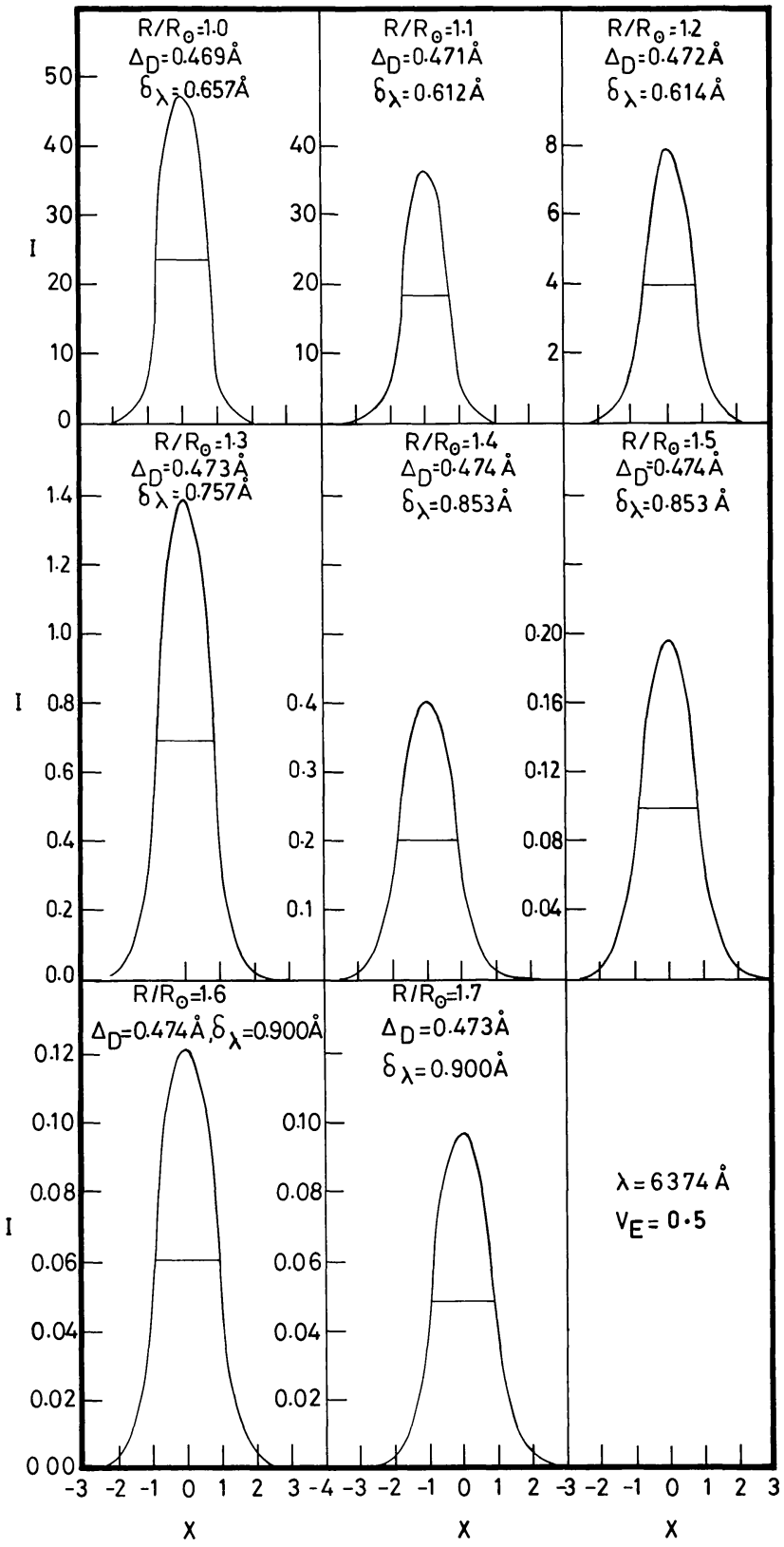

Fig. 11. Same as Figure 10 with V_E = 0.5 Doppler units.

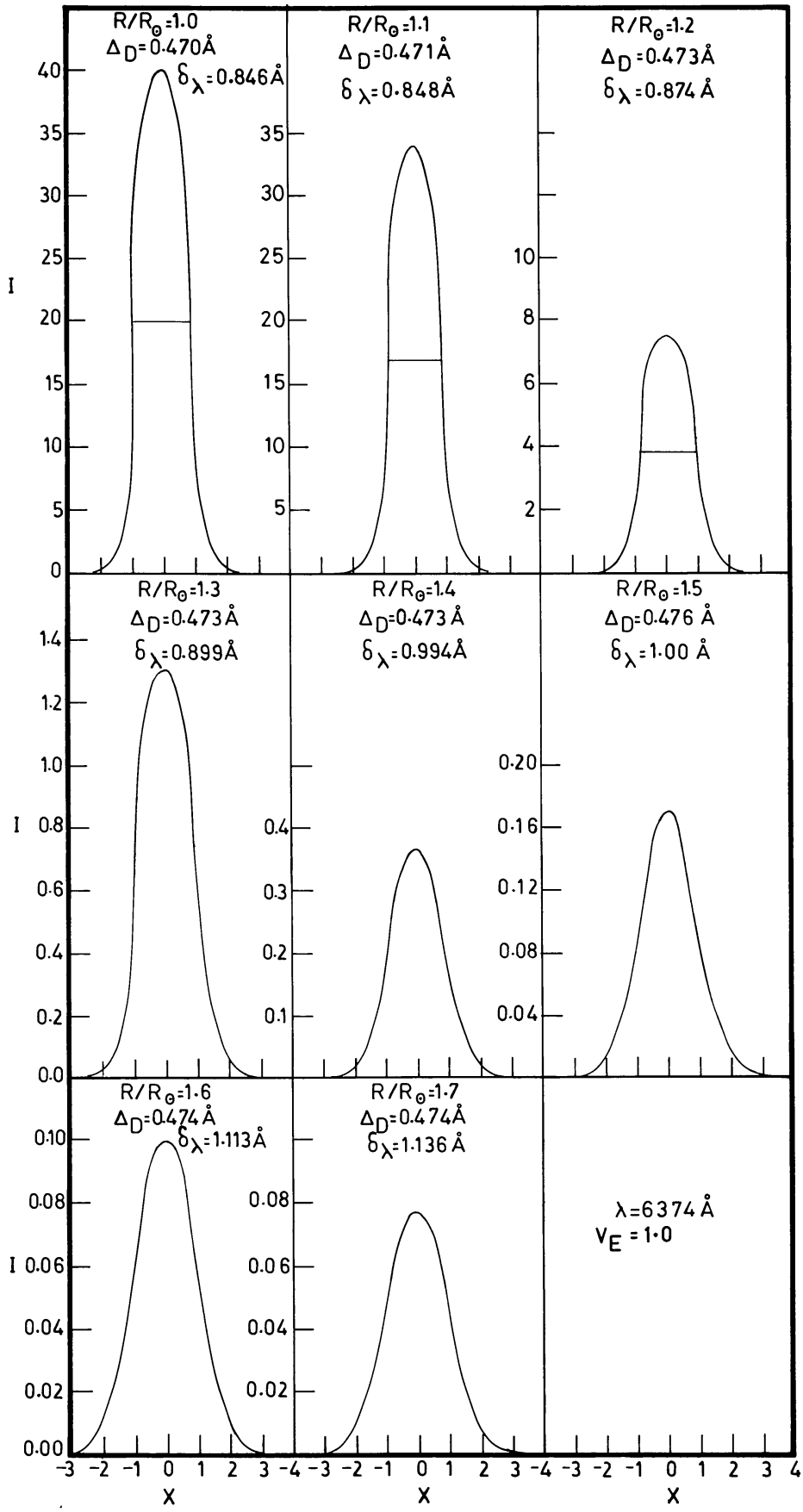

Fig. 12. Same as Figure 10 with V_E = 1.0 Doppler units.

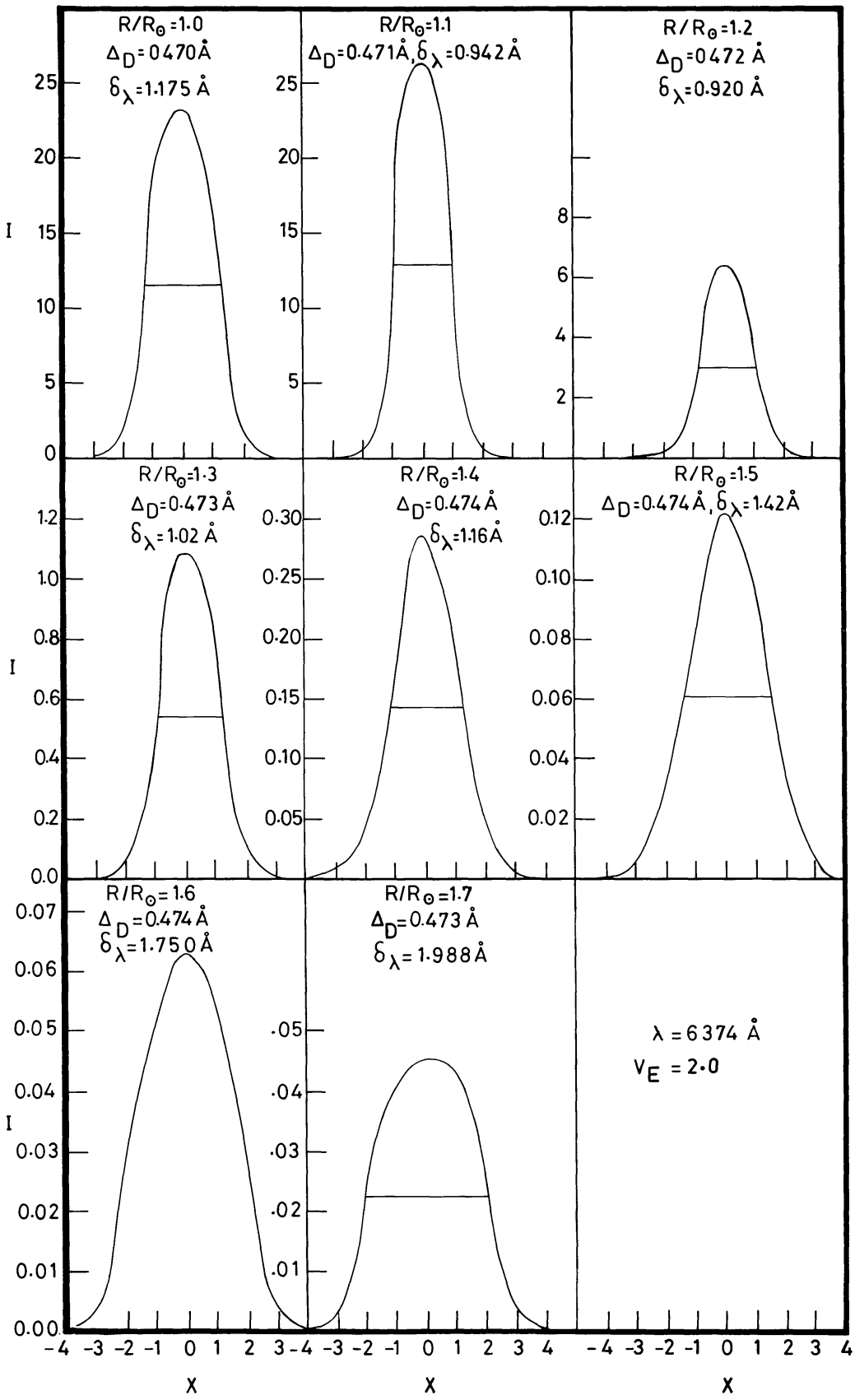

Fig. 13. Same as Figure 10 with $V_E = 2.0$ Doppler units.

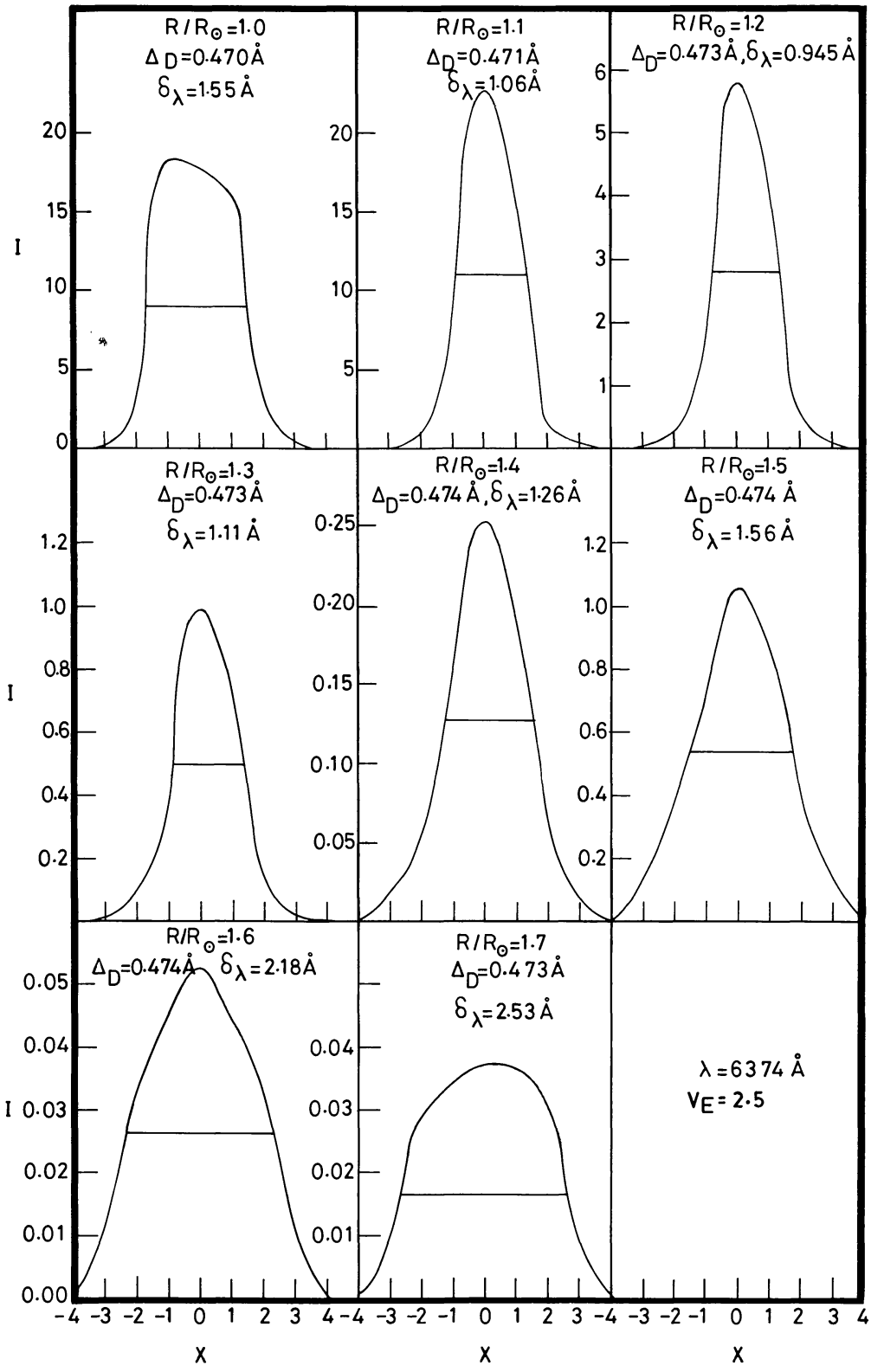

Fig. 14. Same as Figure 10 with V_E = 2.5 Doppler units.

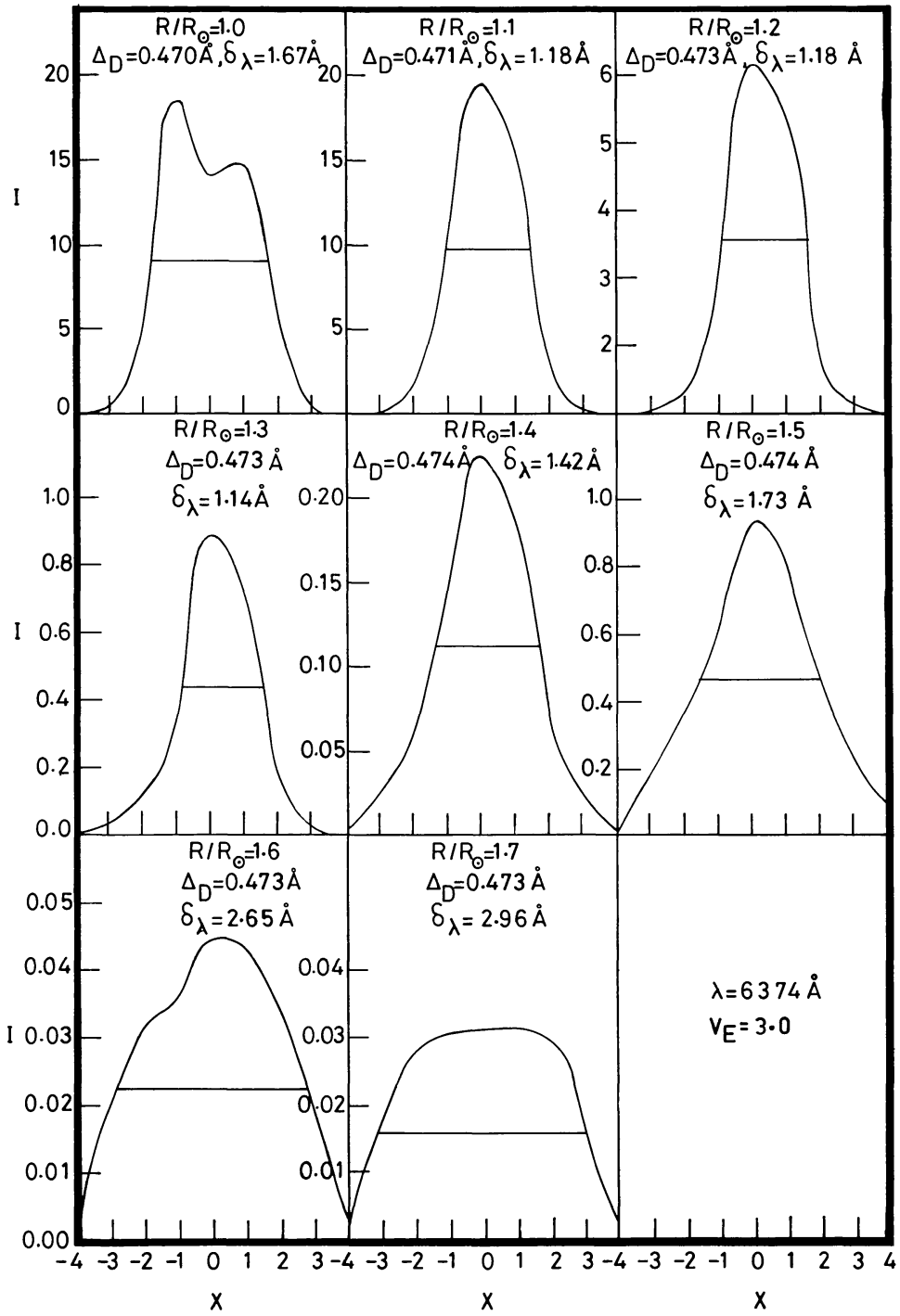

Fig. 15. Same as Figure 10 with V_E = 3.0 Doppler units.

Figures 8 and 9, respectively. It should be mentioned here that we assumed a velocity of expansion V_E which is constant throughout the line-forming region of the corona. This violates the principle of mass conservation in a spherically-symmetric steady-state corona. We assumed a constant velocity of expansion for the sake of simplicity as this is a preliminary study. When $V_E = 0.5\Delta_D$ the widths increased marginally, but when

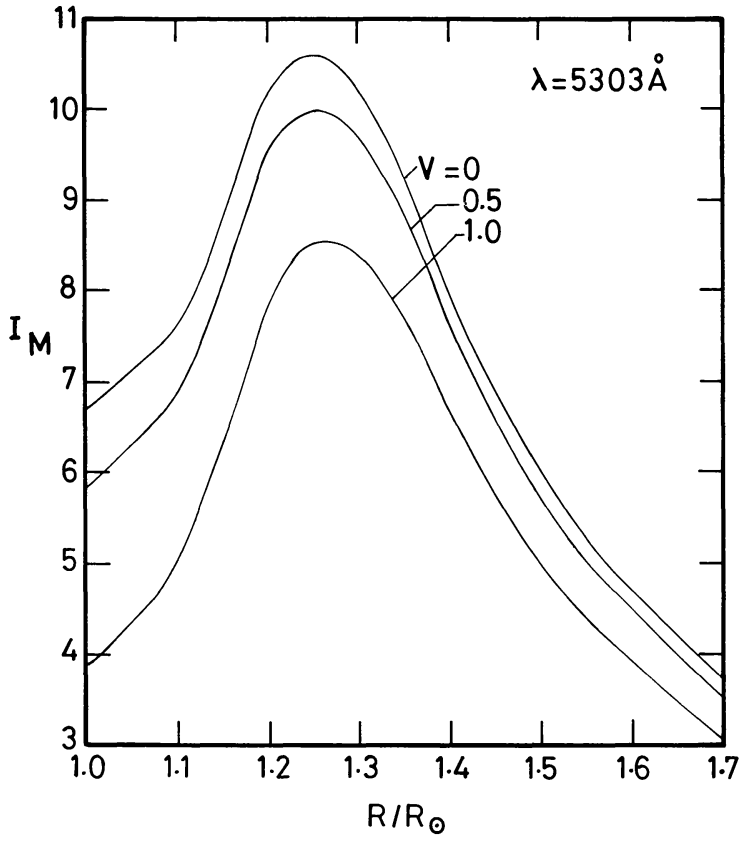

Fig. 16. Variation of the peak emission I_M of the lines versus $R/R_\odot$ for λ5303 Å. The intensities are in arbitrary units.

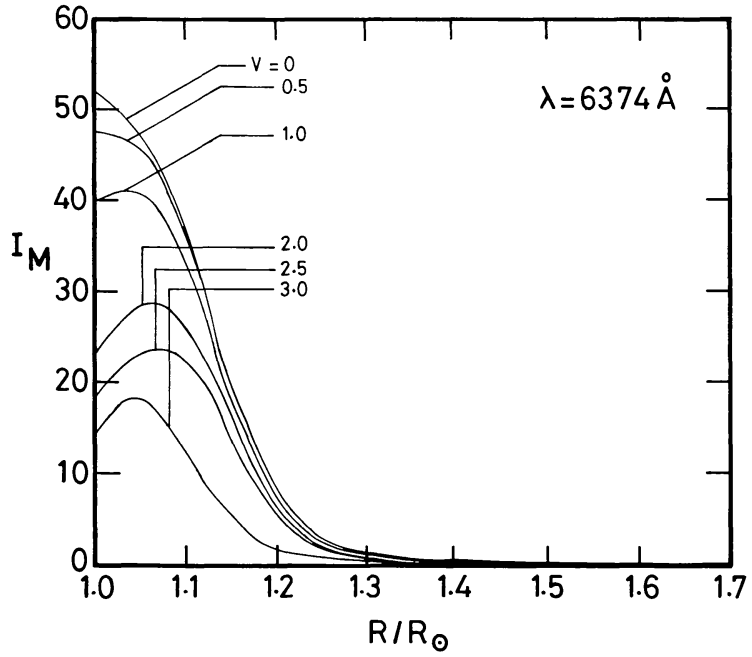

Fig. 17. Same as Figure 16 for λ6374 Å.

$V_E = \Delta_D$ (in Figure 9) we obtain a maximum width of 1.172 Å and a minimum of 0.788 Å. This is an excellent agreement with the observed values given in Figure 1.

In Figure 10, we presented the profiles and δ_λ's corresponding to Fe X ion of 6374 Å emerging out of static corona. A comparison of the widths and profiles in Figure 10 and those given in Figure 2, would reveal that the static corona will not be able to produce such large widths as observed. Therefore, in the subsequent figures (11, 12, 13, 14, 15) we gradually increased the expansion velocity. At about $V_E = 2\Delta_D$ or $3\Delta_D$, we obtain the widths which correspond to those observed given in Figure 2. At $R/R_\odot \geq 1.6$, the width exceeds 2 Å when the V_E equal to $2\Delta_D$. This is also in good agreement with the observations shown in Figure 4 of Singh, Bappu, and Saxena (1982). When $V_E = 3\Delta_D$, the lines show good amount of asymmetry.

In Figures 16 and 17, we plotted the maximum emission I_M of each line at different radial point, in the case of 5303 Å the lines has a peak intensity at about $R/R_\odot \sim 1.25$ while in the case of λ6374 Å the peak intensity can occur at any radial point $1 < R/R_\odot < 1.075$ depending upon the expansion velocity.

3. Conclusions

The emission line profiles of λ5303 Å (Fe XIV) and λ6374 Å (Fe X) in the corona observed at the time of total solar eclipse have been computed. The computed full widths at half maximum of these two emission lines appear to be in good qualitative agreement with those observed. We have made the following assumptions:

(a) a constant velocity of expansion is assumed;

(b) a two-level atom approximation is employed; and

(c) turbulence is not assumed to be the cause of broadening of the lines.

The assumption (a) would imply the violation of the law of conservation of mass according to which the velocity of expansion should vary as $1/r^2$ provided the density remains constant in a steady-state condition. In a real situation we must take into account of the full mass conservation equation. Since the solar wind is not spherically symmetric as shown by several measurements, this does not appear to be a tight constraint and the calculations presented here show some insight on the divergence of the solar wind stream lines. As we have obtained a reasonable agreement with the observations by using a constant velocity law, then the question arises whether or not the stream lines diverge radially from the centre of the Sun or diverge at a lower rate or even slightly converge. However, the full problem can be solved only when the full equation of conservation of mass is solved. Our present calculations also show that turbulence need not be introduced to explain the FWHM in these lines.

The assumption (b) is also not fully consistent but has been employed only to get some physical insight into the problem. One must use the full statistical equilibrium equations to obtain the level populations. These are under study.

Acknowledgements

We would like to thank Dr Jagdev Singh for supplying Figures 1 and 2 and to Dr P. K. Raju for several discussions. We also thank the referee for many useful comments.

References

Allen, C. W.: 1973, *Astronomical Quantities*, The Athlone Press, University of London.
Aller, L. H.: 1963, *The Atmospheres of the Sun and Stars*, Ronald Press Co., New York.
Chandrasekhar, T., Desai, J. N., and Angreji, P. D.: 1981, *Appl. Optics* **20**, 2172.
Desai, J. N. and Chandrasekhar, T.: 1983, *J. Astrophys. Astron.* **4**, 65.
Jordan, C.: 1969, *Monthly Notices Roy. Astron. Soc.* **142**, 501.
Mason, H. E.: 1975, *Monthly Notices Roy. Astron. Soc.* **170**, 651.
Mihalas, D.: 1978, *Stellar Atmospheres II*, Freeman, New York.
Newkirk, 1967: *Ann. Rev. Astron. Astrophys.* **5**, 213.
Peraiah, A.: 1980, *J. Astrophys. Astron.* **1**, 17.
Raju, P. K.: 1985, private communication.
Rybicki, G.: 1970, in H. G. Groth and P. Wellmann (eds.), *Spectrum Formation in Stars with Steadystate Extended Atmospheres*, NBS Special Publication, p. 332.
Singh, J.: 1984, PhD. Thesis (Punjabi University, Patiala) unpublished.
Singh, J., Bappu, M. K. V., and Saxena, A. K.: 1982, *J. Astrophys. Astron.* **3**, 249.
Traving, G.: 1975, in B. Baschek, W. H. Kegel, and G. Traving (eds.), *Problems in Stellar Atmospheres and Envelopes*, Springer-Verlag, Berlin.